# Identification of Network Dynamics and Disturbance for a Multi-zone Building \*

Tingting Zeng \* Prabir Barooah \*\*

\* Department of Mechanical and Aerospace Engineering, University of Florida, Gainesville, FL, 32611 USA (e-mail: tingtingzeng@ufl.edu).

**Abstract:** We propose a method that simultaneously identifies a sparse transfer matrix and disturbance for a multi-zone building's dynamics from input-output measurements. An  $\ell_1$ -regularized least-squares optimization problem is solved to obtain a sparse solution, so that only dominant interactions among zones are retained in the model. The disturbance is assumed to be piecewise-constant: the assumption aids identification and is motivated by the nature of occupancy that determines the disturbance. Application of our method on data from a simulation model shows promising results.

*Keywords:* system identification,  $\ell_1$ -penalty, sparsity, disturbance, MIMO system

## 1. INTRODUCTION

Heating, ventilation, and air conditioning (HVAC) systems in buildings have a significant impact on energy consumption. Buildings consume 27% of the total energy delivery in the United States in 2017 United States Energy Information Administration (2018), and HVAC systems account for about half of the energy consumed in commercial buildings Energy Information Administration (2012). The HVAC system of a building is also responsible for the quality of the indoor climate, which directly affects health and comfort of occupants Tom (2008); Fisk (2000). There has been a significant amount of interest in recent years to improve energy efficiency of buildings through advanced control methods. Occupant comfort and health serves as important constraints to the control objective: comfort plays a crucial role in determining productivity Seppänen et al. (2005); Sensharma et al. (1998);

More recently there is renewed interest in providing occupants of office buildings *personalized comfort*. Individuals differ in their perceptions of thermal comfort ASHRAE (2009); Schellen et al. (2012). Ideally the thermal and air quality measure of each occupant's space should be controlled to meet that particular individual's preference. Products such as comfy<sup>TM</sup>(www.comfy.app) are examples of such efforts. In these applications, energy use may serve as a constraint rather than being the objective.

Advanced control of HVAC systems need a low-order model relating the inputs to outputs. For a modern commercial building equipped with variable air volume (VAV) systems, control inputs may include rate of airflow and rate of cooling/heating. Relevant outputs include temperature at a minimum, but can also include humidity, concentration of pollutants etc. In this paper we consider temperature as the output, and denote by "zone" a space whose temperature has an impact on at least one occupant's comfort and health.

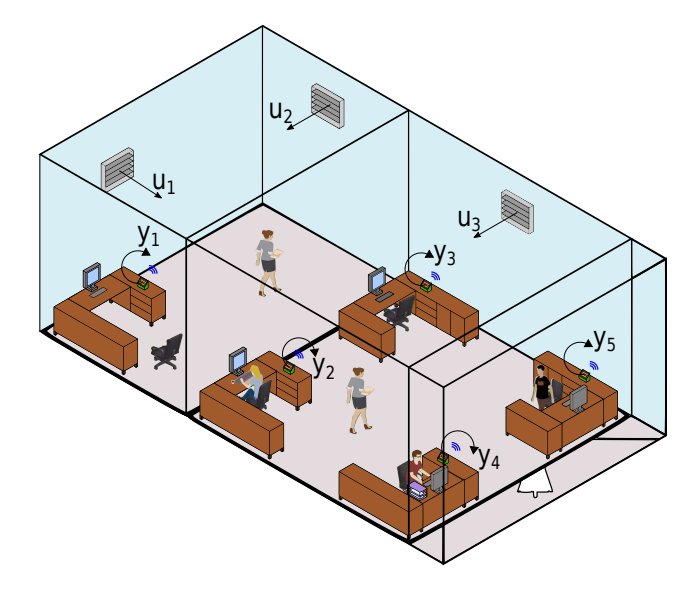


Fig. 1. An example of a building layout with multiple inputs and outputs.

The complexity of the physical processes that determine the input-output behavior makes control-oriented modeling a challenging task. The modeling problem gets exacerbated when one considers an open-plan office, or a building in which there are considerable thermal interactions among the zones, such as the one shown in Figure 1. Due to inter-zone thermal interaction, each actuator (VAV box) may impact several outputs (temperatures at several zones).

This paper is about identifying control-oriented models of multi-zone buildings from measurements of inputs and outputs. It is envisioned that the identified models will be used for predictive control to provide higher energy efficiency and/or personalized comfort, though the control design problem is outside the scope of this paper. A data-driven approach is chosen over a physics-based approach for modeling because of the complexity of the underlying physics.

<sup>\*\*</sup> Department of Mechanical and Aerospace Engineering, University of Florida, Gainesville, FL, 32611 USA (e-mail: pbarooah@ufl.edu)

<sup>\*</sup> This research is partially funded by the National Science Foundation (award # 1463316) and a Renewable Energy and Energy Efficient Technologies (REET) grant from the Florida Department of Consumer Services.

A key bottleneck in data-driven identification of thermal models of buildings is the presence of large exogenous disturbances (various unknown heat gains). The thermal energy expended by the HVAC system is mostly spent to reject these disturbances; hence these disturbances cannot be assumed to be small. Even without inter-zone interactions, presence of unknown disturbances has been a bottleneck in identifying dynamic models of single-zone building models. Only recently this issue has been addressed in a principled manner; see Penman (1990); Wang and Xu (2006); Kim et al. (2016); Zeng et al. (2017); Coffman and Barooah (2018). These papers are limited to single zones.

The problem we seek to address is that of simultaneously identifying (1) a multiple-input multiple-output (MIMO) transfer matrix - the plant - and (2) the exogenous disturbances, from measurements of inputs and outputs. The transfer matrix can be visualized as a bipartite graph, with edges from the input nodes to output nodes; see Figure 2. We seek to identify a *sparse graph* with a small number of edges. It is hoped that a sparse model will retain information of only the dominant interactions, and thereby help control computations.

Because of the unknown disturbances, the problem is not well-posed: there are infinitely many possible pairs of plant models and disturbance signals that will produce the same output signals. To make the problem well-posed, we assume that the exogenous disturbances are piecewise - constant, so that their derivatives are sparse signals, i.e., mostly zero. The piecewise-constant assumption is motivated by the fact that the exogenous disturbances consist of heat gains from occupants' bodies and equipments such as computers and printers. Since these heat gains are highly correlated to occupancy, and occupancy varies in an approximately piecewise-constant manner, so should these heat gains Coffman and Barooah (2018). The sparsity constraint limits the number of possible disturbance signals that fit the data. In addition, since the graph relating inputs to outputs is also sought to be sparse, sparsity provides an unifying theme.

The identification problem is posed as an  $\ell_1$ -regularized least squares problem; the  $\ell_1$  penalty promotes a sparse solution. Recent years there has been an explosion in both theory and applications of sparse signal recovery by using an  $\ell_1$  penalty; see James et al. (2014); Hayden et al. (2016); Yue et al. (2017) and references therein.

While there are a number of papers on the problem of modeling multi-zone building dynamics (see Atam and Helsen (2016); Goyal et al. (2011); Doddi et al. (2018) and references therein), to the best of our knowledge the only reference that simultaneously identifies a plant model and disturbance for a multi-zone building is the recent reference by Kim *et al.* Kim et al. (2017). Their method, which requires solving a non-convex problem, estimates the plant parameters and an output disturbance (a disturbance that is added to the plant output) that encapsulates the effect of an unknown input disturbance. The method results in a complete interaction model connecting each input-output pair. In contrast, the method proposed here involves convex optimization and results in a sparse interaction model.

A body of work that is closely related to this paper is the growing literatures on network structure identification. Some of these papers are concerned with the blind identification problem in which input measurements are not available, only output measurements are; see Materassi et al. (2013) and

references therein. A paper that is closer in spirit to the current work is Yue et al. (2017) in which a sparse network structure is identified based on input-output measurements. However, Yue et al. (2017) only dealt with the problem of determining the binary structure of the graph (presence or absence of an edge), whereas our work addresses the additional problem of identifying the transfer function associated with each edge. A major difference between the current work and all previous works on network structure identification is that none of those papers contended with the *simultaneous identification of plant and disturbance* problem we are dealing with.

The rest of the paper is organized as follows. Section 2 formulates the problem precisely, Section 3 describes the proposed algorithm, and Section 4 describes evaluation results when the algorithm is applied to simulation data. The paper concludes with some comments in Section 5.

## 2. PROBLEM FORMULATION

The *output node set*, denoted by  $\mathcal{V}_y$ , is the locations with temperature sensors whose measurements are outputs of the model we wish to identify. The number of *output nodes* is denote by  $n_y$  (=  $|\mathcal{V}_y|$ ,  $|\cdot|$  denotes cardinality). The *input node set*  $\mathcal{V}_u$  contains the set of controllable inputs (VAV boxes), and the set of exogenous inputs (outside air temperature and solar irradiance). Figure 4 shows a schematic of an openplan building; it has 6 input nodes (4 VAV boxes, outside air temperature and solar irradiance) and 10 output nodes (10 zones in total: 8 cubicles and 2 conference rooms).

Time is measured by a discrete counter  $k=0,1,2,\ldots$  At time k, let  $y_i[k]\in\mathbb{R}$  be the measured air temperature at node  $i,\ u_j[k]$  be the three known inputs : (1) the rate of heat gain due to the air supply,  $q_{\mathrm{hvac}}(\mathrm{kW})$ , (2) the outside air temperature  $T_{oa}$  (°C), (3) the solar irradiance  $\eta^{\mathrm{sol}}(\mathrm{kW/m^2})$ , and  $w_i[k]$  be the unknown disturbance (total heat gain due to occupants, plug loads etc.), at output node i. We denote  $y[k] = [y_1[k], y_2[k], \ldots, y_{n_y}[k]]^T, u[k] = [u_1[k], u_2[k], \ldots, u_{n_u}[k]]^T,$  and  $w[k] = [w_1[k], w_2[k], \ldots, w_{n_y}[k]]^T.$ 

Our starting point is a MIMO (multiple-input-multiple output) transfer matrix in Z-transform domain:

$$Y(z^{-1}) = G_u(z^{-1})U(z) + G_w(z^{-1})W(z^{-1})$$

$$= \frac{1}{D(z^{-1})} \left( N_u(z^{-1})U(z^{-1}) + N_w(z^{-1})W(z^{-1}) \right)$$

$$= \frac{1}{D(z^{-1})} \left( N_u(z^{-1})U(z^{-1}) + \bar{W}(z^{-1}) \right),$$
(1)

with  $Y, \bar{W} \in \mathbb{C}^{n_y}, G_u, N_u \in \mathbb{C}^{N_y \times N_u}, D \in \mathbb{C}, G_w, N_w \in \mathbb{C}^{N_y \times N_y}$ , where the second equality is obtained by making  $D(z^{-1})$  the least common multiple of the denominators of  $G_u(z^{-1})$  and  $G_w(z^{-1})$ , and the third equality is obtained by defining  $\bar{W}(z^{-1}) := N_w(z^{-1})W(z^{-1})$ . Here we assume  $N_w$  is diagonal, meaning output  $y_i$  is only affected by disturbance  $w_i$ . Denote  $\rho$  as the order of  $D(z^{-1})$ , then,

$$D(z^{-1}) = 1 - \sum_{k=1}^{\rho} \theta_k z^{-k}$$

$$N_u(z^{-1}) = \begin{bmatrix} \dots & \dots & \dots \\ \vdots & \sum_{k=0}^{\rho} \theta_{(n_u(i-1)+j)(\rho+1)+k} z^{-k} & \vdots \\ \dots & \dots & \dots \end{bmatrix}$$

$$\bar{W}(z^{-1}) = \begin{bmatrix} \vdots \\ N_{w_i}(z^{-1}) w_i(z^{-1}) \\ \vdots & \vdots \end{bmatrix}$$

for some plant parameters  $\theta_k$ 's.

The interactions captured by the transfer matrix model described above can be visualized by a graph  $\mathcal{G}=(\mathcal{V},\mathcal{E})$  with node set  $\mathcal{V}=\mathcal{V}_u\cup\mathcal{V}_y$  and edge set  $\mathcal{E}\subset\mathcal{V}_u\times\mathcal{V}_y$ . An edge e=(i,j) from  $j\in\mathcal{V}_u$  to  $i\in\mathcal{V}_y$  exists if and only if  $N_{ji}(z)\neq 0$  for every z. It is a bipartite graph without cycles: an edge is possible between an input node and an output node (sensor) but not between actuator pairs or sensor pairs Diestel (2005). In the extreme case when every actuator affects every sensor, the graph will look like what is shown in Figure 2. In practice the graph will be far more sparse, an actuator will only have an affect on a small number of sensors.

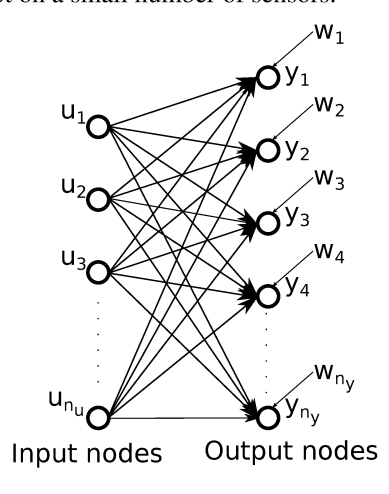


Fig. 2. The most general case of the network structure of a multi-zone HVAC model: a complete directed bipartite graph without cycles, with an edge from every input node to every output node.

Following assumptions are made to reduce the number of free parameters.

Assumption 1. Define 
$$w_{bldg}[k] := \sum_{i=1}^{n_y} w_i[k]$$
,  $\exists k_w = [k_w^1, \dots, k_w^{n_y}]^T \in \mathbb{R}^{n_y}, \sum_{i=1}^{n_y} k_w^i = 1$ , such that  $w_i = k_w^i w_{bldg}$ ,  $\forall i = 1, \dots, n_y$ .

Assumption 2.

$$\exists \ N_w^{bldg}, \ s.t. \ N_w^{bldg} = N_{w_i}, \ \forall \ i = 1, \dots, n_y.$$

Then  $\bar{W}(z^{-1})$  can be rewritten as

$$\bar{W}(z^{-1}) = \begin{bmatrix} \vdots \\ k_w^i N_w^{bldg}(z^{-1}) w_{bldg}(z^{-1}) \\ \vdots \end{bmatrix}.$$

Performing an inverse Z-transformation on (1) and defining

$$\bar{w}_{bldg} := Z^{-1} \left( N_w^{bldg}(z^{-1}) w_{bldg}(z^{-1}) \right) \in \mathbb{C}$$
 (2)

as the *transformed* disturbance, yields a difference equation, from which we obtain the linear regression form:

$$y[k] = \Phi[k]\theta, \qquad k = \rho + 1, \dots, k_{max}$$
 (3)

where  $\theta = [\theta_{p_d}^T, \theta_{p_n}^T, \bar{w}_{bldg}^T]^T$ , in which  $\theta_{p_d} = [\theta_1, \dots, \theta_\rho]^T$  are plant parameters that appear in  $D(z^{-1})$ ,  $\theta_{p_n} = [\theta_{\rho+1}, \dots, \theta_{n_y n_u(\rho+1)+\rho}]^T$  are plant parameters that appear in  $N_u(z^{-1})$ , and  $\bar{w}_{bldg} = [\bar{w}_{bldg}[\rho+1], \dots, \bar{w}_{bldg}[k_{max}]]^T$  are the transformed disturbance defined in (2), where  $k_{max}$  is the number of the time indices for which data are collected. Also,

$$\Phi := \begin{bmatrix} \vdots \\ \phi^i \\ \vdots \end{bmatrix}, \quad i = 1, \dots, n_y,$$
$$\vdots \\ \in \mathbb{R}^{n_y(k_{max} - \rho) \times k_{max} + n_y n_u(\rho + 1)}$$

where each block  $\phi^i$  has the form:

$$\phi^{i} = \begin{bmatrix} y_{i}[\rho+1] & \dots & y_{i}[1] & \phi_{u_{1}}^{i} & \dots & \phi_{u_{j}}^{i} & \dots & k_{w}^{i}e_{1} \\ \vdots & & \vdots & & \vdots & & \vdots \\ y_{i}[k] & \dots & y_{i}[k-\rho] & \phi_{u_{1}}^{i} & \dots & \phi_{u_{j}}^{i} & \dots & k_{w}^{i}e_{k-\rho} \\ \vdots & & \vdots & & \vdots & & \vdots \\ & \vdots & & \vdots & & \vdots & & \vdots \end{bmatrix}$$

$$\in \mathbb{R}^{k_{max}-\rho \times k_{max}+n_{y}n_{u}(\rho+1)}, \qquad j=1,\dots,n_{u},$$
(4)

where  $e_k$  is the k-th canonical basis vector of  $\mathbb{R}^{k_{max}-\rho}$  in which the 1 appears in the k-th place, and

$$\phi_{u_j}^i = \left[ 0_{1 \times (\rho+1)(i-1)} \middle| u_j[k] \dots u_j[k-\rho] \middle| 0_{1 \times (\rho+1)(n_y-i)} \right] \in \mathbb{R}^{1 \times n_y(\rho+1)}$$
(5)

Our goal is to identify from measurements of inputs and outputs, (1) a transfer matrix  $G_u(z^{-1})$  that is sparse, meaning its graph has a small number of edges, and (2) the signal  $\{\bar{w}_{bldg}[k]\}$ , so that the resulting model (transfer matrix and transformed disturbance) predicts the output well.

# 3. PROPOSED ALGORITHM

Identifying  $G_u(z^{-1})$  and  $\{\bar{w}_{bldg}(k)\}$  from measurements of u[k],y[k] is an ill-posed problem since an infinite number of solutions to (3) exist. We assume that the transformed disturbance  $\bar{w}_{bldg}[k]$  is piecewise-constant. The motivation behind this assumption is that the disturbance is mostly due to the occupants, and occupancy in commercial buildings can be modeled as a piecewise-constant signal: people come in at a particular time and stay in until workday is over, perhaps leave the building temporarily during lunch. Since the transformed disturbance  $\bar{w}_{bldg}[k]$  is a linear combination of time-shifted value the disturbance  $w_{bldg}[k]$ , the same trend should hold for  $\bar{w}_{bldg}[k]$ . The derivative of such a signal is sparse, i.e., mostly zero. Therefore we seek a piecewise-constant  $\bar{w}_{bldg}$  by penalizing the  $\ell_1$ -norm of the derivative of  $\bar{w}_{bldg}$ . The discrete time derivative is  $D_1\bar{w}_{bldg}$ , where  $D_1 \in \mathbb{R}^{k_{max}-\rho-1 \times k_{max}-\rho}$  is the first difference matrix:

$$D_{1} := \begin{bmatrix} -1 & 1 & 0 & \dots & \dots \\ 0 & -1 & 1 & 0 & \dots \\ & & \ddots & \ddots & \\ & & \ddots & \ddots & \\ \dots & \dots & 0 & -1 & 1 \end{bmatrix}.$$
 (6)

In addition, a sparse reconstruction of transfer matrix  $G_u(z^{-1})$  can be promoted by penalizing the  $\ell_1$ -norm of  $\theta_{p_n}$ , the vector of the coefficients that determines the numerator matrix  $N_u(z^{-1})$ . Note that the parameters that determine the denominator  $D(z^{-1})$  need not to be sparse. Let  $S \in \mathbb{R}^{(\rho+1)(n_yn_u-1)+k_{max}\times(\rho+1)n_yn_u+k_{max}}$  be defined as

$$S := \left[ \left. \begin{matrix} 0_{(\rho+1)(n_yn_u-1)+k_{max}\times\rho} \middle| \begin{matrix} I_{(\rho+1)n_yn_u} \middle| 0 \\ 0 \end{matrix} \middle| D_1 \end{matrix} \right],$$

so that

$$(S\theta)^T = [\theta_{p_n}^T, D_1 \bar{w}_{bldq}^T].$$

We now pose the following optimization problem to estimate the plant transfer matrix and a transformed disturbance:

$$\hat{\theta} = \arg\min_{\theta} \frac{1}{2} \|y - \Phi\theta\|_2^2 + \lambda \|S\theta\|_1, \tag{7}$$

which is called "generalized Lasso" Ali and Tibshirani (2018). Here  $\lambda>0$  is an user-defined weight, which is crucial in determining the solution to (7). A larger  $\lambda$  will make the resulting  $S\theta$  sparser. In order to illustrate the choice of  $\lambda$ , first we need to draw some connections with the "standard Lasso" problem, which is:

$$\hat{\chi} = \arg\min_{\chi} \frac{1}{2} \| \boldsymbol{z} - \Psi \chi \|_{2}^{2} + \lambda \| \chi \|_{1}.$$
 (8)

## 3.1 Regularization Parameter Selection

Two common heuristics for choosing  $\lambda$  for the standard Lasso problem (8) are cross-validation Pendse (2011) and L-curve-based curvature methods Hansen (1992). However, neither of them is applicable to our problem as they have implementation requirements that our problem does not satisfy.

Cross validation divides datasets into K folders and requires that parameters to be retrieved are the same among such folders, whereas parameters in our problem contain transformed disturbance, which may differ from one day to the next. The L-curve, which is a "log-log" plot of the norm of a regularized solution  $\|\chi\|_1$  versus the norm of the corresponding residual norm  $\|z-\Psi\chi\|_2$ ", can graphically display the trade-off between the size of a regularized solution and its fit to the given data, where optimal regularization parameter that minimize the trade-off lies at the corner of such L-curve. For the L-curve method, a solution path that changes monotonically with respect to  $\lambda$  is essential, i.e.,  $(\Psi^T\Psi)^{-1}$  in (8) needs to be diagonally dominant Duan et al. (2016). That is also not satisfied in our case.

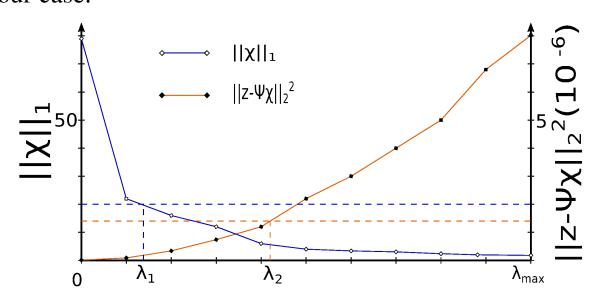


Fig. 3. Illustration of regularization parameter selection

We use the following heuristic to choose  $\lambda$ , which is inspired by the L-curve method. First, we plot both the solution norm and residual norm individually against  $\lambda$  by repeatedly solving Problem (7) for  $\lambda \in [0, \lambda_{max}]$ , where  $\lambda_{max}$  is a sufficiently large value. An illustration of these two plots is shown in

Figure 3. Second, we identify a value  $\lambda_1$  so that the solution norm is smaller than a user-defined threshold for any  $\lambda > \lambda_1$ , and then identify  $\lambda_2$  so that the residual norm is smaller than a user-defined threshold for any  $\lambda < \lambda_2$ . If  $\lambda_2 > \lambda_1$ , choose  $\lambda$  to be  $\lambda_1$ . If not, pick another threshold, and continue until this condition is met.

Notice that  $\lambda$  in (7) and (8) are identical, that is,  $\lambda$  determined from (8) can be directly used in (7).

The optimization problem (7) is convex. All numerical results presented in this paper are obtained by using the cvx package for solving convex problems in MATLAB<sup>©</sup> Grant and Boyd (2011).

## 4. EVALUATION

A numerical experiment is conducted in order to test the proposed method. We perform simulations on a coupled ODE model of a multi-zone building, and then test the method on the resulting data. The model used for simulating a building will be called "virtual test building" in the sequel. Considering a 6th order model is with the lowest order that can have distinct time-constant for each input, hence we test the method with  $\rho=6$ .

#### 4.1 Virtual Building Description

The floor plan of the virtual building is shown in Figure 4. A RC (resistor-capacitor) network model is used as the virtual

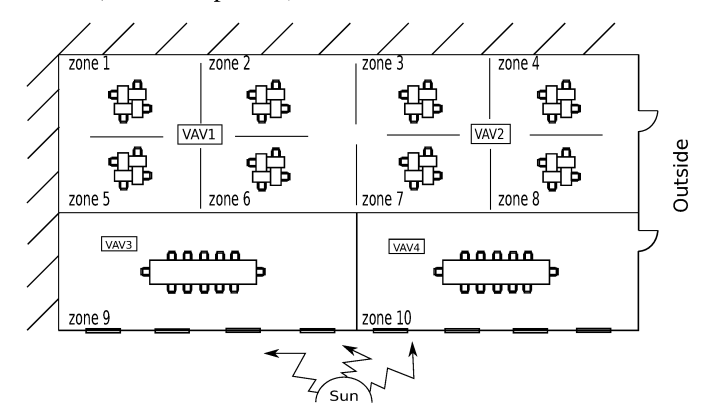


Fig. 4. Floor plan of the virtual building used to generate data: VAV boxes 1 and 2 directly deliver air to each of the four nearby zones while VAV boxes 3 and 4 only deliver to zones 9 and 10, respectively.

building as shown in Figure 5. RC network model is a common modeling paradigm for building thermal dynamics Madsen and Hoist (1995). The parameters of the model were chosen in the following manner. The RC network model of a single zone that was obtained by calibration with data collected from a zone in a building at the University of Florida campus (Pugh Hall) were chosen first Coffman and Barooah (2018). This single zone model has two C's and two R's. For each of the eight smaller zones in the virtual building, these same R's and C' are chosen. For the two larger zones, the C's are chosen as three times these values and R's as one thirds. Other parameters are chosen the same as in Coffman and Barooah (2018). The virtual building is a set of coupled ODEs with 15 states (10 measurable temperatures, one for each output node, and 5 unmeasurable temperatures at 5 inter-connecting points of output

nodes), 6 inputs (4 controllable heat gains from HVAC system, ambient temperature, and solar irradiance) and 10 exogenous disturbances, one for each zone. The input signals are chosen

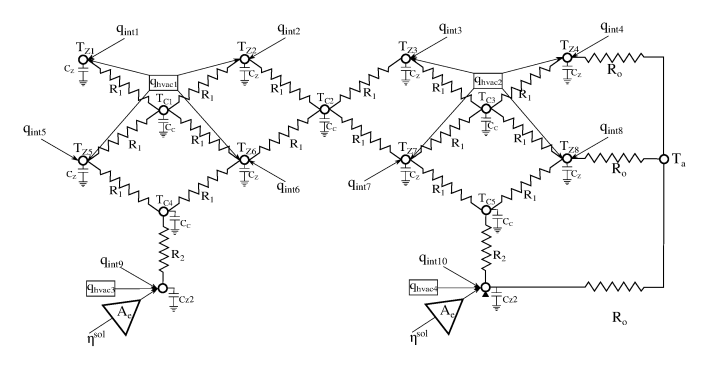


Fig. 5. A schematic of the "RC" network model that constitutes the virtual building.  $q_{int}$ 's are the "internal heat gain", i.e., the disturbances.  $A_e$  is the effective area.

as follows: the input component  $q_{\rm hvac}$  is chosen by scaling a measured data from Pugh Hall, and is shown in Figure 6. Ambient temperature is taken from weatherunderground. com, and solar irradiance data is taken from NSRDB: https://nsrdb.nrel.gov/, both for Gainesville, FL, and are shown in Figure 6 (bottom). Disturbances are chosen somewhat arbitrarily, by scaling  $CO_2$  data from Pugh Hall, and are shown in Figure 7. The disturbances are chosen arbitrarily without satisfying the Assumption 1. The sampling time for this experiment is 5 minutes.

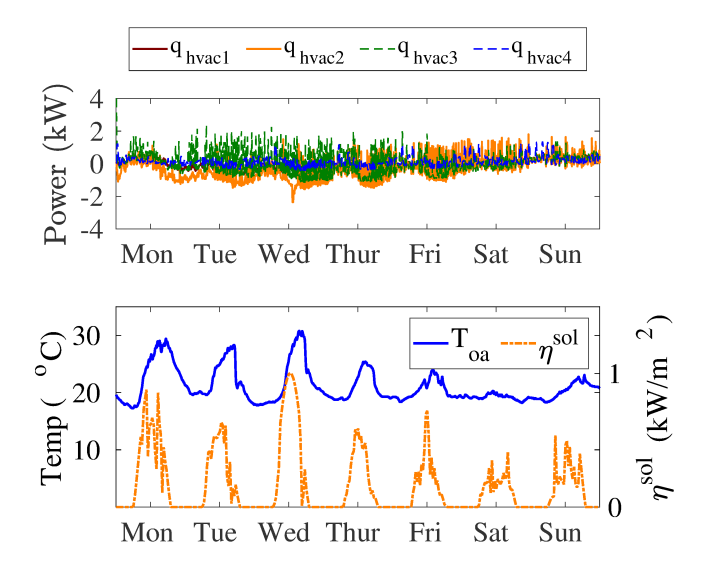


Fig. 6. Input-output data used for algorithm evaluation.

#### 4.2 Evaluation Results

Zone Temperature Prediction The identified transfer matrix and transformed disturbance are used to predict zone temperatures. Table 1 shows the RMS values of the prediction errors for each zone. The maximum RMS value is  $0.439^{\circ}$ C, which occurs in zone 1. Figure 8 shows the measured and predicted temperature for this zone.

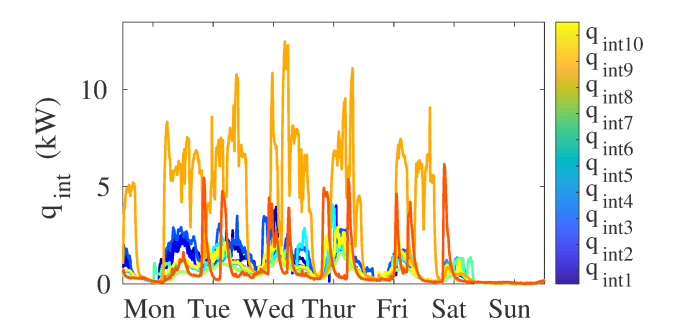


Fig. 7. Disturbance data for algorithm evaluation. Notice  $w_i \neq k_w^i w_{bldq}$ .

Table 1. RMS values of the zone temperature prediction error (°C).

zone 1	zone 2	zone 3	zone 4	zone 5
0.439	0.345	0.405	0.334	0.277
zone 6	zone 7	zone 8	zone 9	zone 10
0.253	0.191	0.201	0.363	0.288

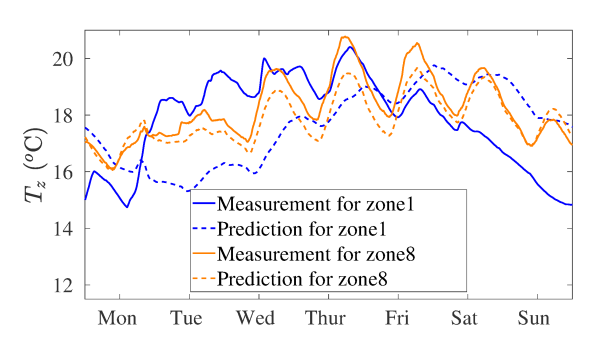


Fig. 8. Evaluation: temperature measurement and prediction for zone 1.

Plant/network identification Comparison of identified transfer matrix with the ground truth can be done in a straightforward manner by comparing the frequency responses. But this method is cumbersome due to the large number of input-output pairs (a total of 60). In addition, it does not help visualizing the sparsity of the identified model  $\hat{G}_u$  or the ground truth  $G_u$ . Another issue is that the entries of the transfer matrix of neither the virtual building nor the identified model will be strictly zero. There are no zero entries in  $G_u(z^{-1})$  due to the interaction among states of the virtual building, which makes every entry of  $G_u(z)$  non-zero. As for the identified model  $\hat{G}_u(z^{-1})$  that is constructed from  $\hat{\theta}$ , finite-precision numerical calculations cause the entries of  $\hat{\theta}$  to be non-zero.

In view of the above, a transfer matrix is visualized through the total energy of impulse response of  $G_{p\ell}(z^{-1})$ , which is a measure of gain between input-output pair  $u_\ell$  and  $y_p$ . Denoting by  $g_{p\ell}[k]$  the impulse response, we define

$$E_{G_{p\ell}} := \sum_{0}^{\infty} |g_{p\ell}[k]|^2 = \frac{1}{2\pi} \int_{0}^{2\pi} |X(e^{j\Omega})|^2 d\Omega$$

where the equality follows from Perseval's relation Oppenheim et al. (1997). When the integral is computed from the identified transfer matrix elements, it is denoted as  $E_{\hat{G}_{p\ell}}$ .

Figure 9 shows the resulting comparison of the heat map between  $E_{G_{ij}}$  and  $E_{\hat{G}_{ij}}$ . Markers with darker color represent

higher energy. The strength of input-output interactions we see from Figure 9 are consistent with what we expect from the building layout shown Figure 4. For instance, VAV box 1 supplies air to zones 1,2,5,6, so  $u_1$  should have a strong impact on  $y_1,y_2,y_5,y_6$ , while its effect on the other outputs are expected to be weak. Similar trends are also observed for the other inputs from VAV boxes. The pairs i,j in which  $E_{G_{ij}}$  is non-zero,  $E_{\hat{G}_{ij}}$  are also non-zero.

These results indicate the proposed algorithm is able to identify dominant network interactions quite accurately. The estimated transfer functions from exogenous inputs  $u_5$  ( $T_a$ ) and  $u_6$  ( $\eta^{\rm sol}$ ) are less accurate than from the controllable inputs, in terms of the gain  $E_{G_{ij}}$ . We believe it is because of lack of adequate excitation in the data for the exogenous inputs; see Figure 6.

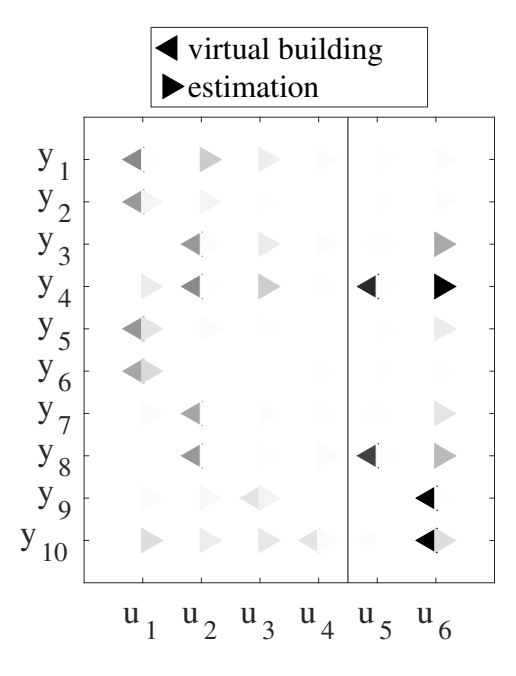


Fig. 9. Evaluation: comparison of the heat map between the  $E_{G_{ij}}$  and  $E_{\hat{G}_{ij}}$ : markers shown in darker color represent higher energy, and empty slots correspond to SISO transfer functions that are 0.

Disturbance There is no ground truth  $\bar{w}_{bldg}[k]$  that can be compared to the estimated  $\hat{w}_{bldg}$  since Assumptions 1 and 2 are not satisfied in the virtual building. We therefore compare the estimated transformed disturbance,  $\hat{w}_{bldg}$ , with the "total building disturbance" defined as  $w_{bldg}[k] := \sum_{i=1}^{i=n_y} w_i[k]$ . Figure 10 shows a comparison between  $w_{bldg}$  and  $\hat{w}_{bldg}$ , which shows that the signals are highly correlated. In fact, the covariance between these two time series is 0.821. This is quite high since  $\hat{w}_{bldg}$  is an estimate of a linear transformation of the disturbance, not of the disturbance itself.

# 5. CONCLUSION

We proposed an algorithm to simultaneously identify a MIMO transfer matrix of a multi-zone building, and a transformed version of the building-wide exogenous disturbance, by solving a convex optimization problem. An  $\ell_1$ -regularized least-squares problem is posed to promote a solution that leads to a sparse

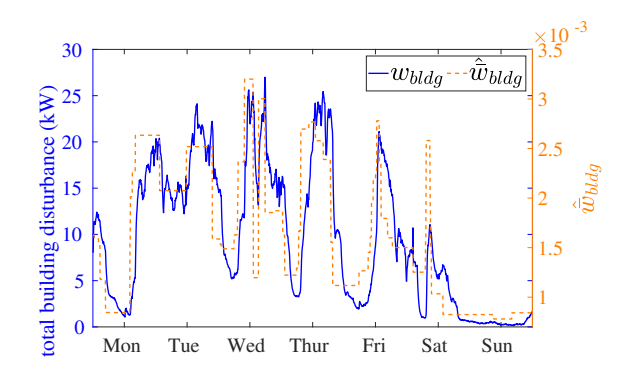


Fig. 10. Evaluation: comparison between total building disturbance and estimated transformed disturbance.

network structure and a transformed disturbance signal. Application of the method to simulation generated data shows that it is able to recover a sparse transfer matrix and a piecewise-constant transformed disturbance that accurately predict zone temperatures. The identified transformed disturbance is highly correlated to the true disturbance, providing confidence in the ability of the method to obtain a meaningful disturbance estimate.

There are several avenues for future work. The first is application of the method to data from real buildings. The challenge here is evaluation, since there is no ground truth to compare to. Another area is the identification of the disturbance. The proposed method only identifies a transformed disturbance, which is related to the disturbance by a non-invertible linear transformation.

#### **REFERENCES**

Ali, A. and Tibshirani, R.J. (2018). The generalized lasso problem and uniqueness. *arXiv preprint arXiv:1805.07682*. ASHRAE (2009). The ASHRAE handbook fundamentals (SI Edition).

Atam, E. and Helsen, L. (2016). Control-oriented thermal modeling of multizone buildings: methods and issues: intelligent control of a building system. *IEEE Control Systems*, 36(3), 86–111.

Coffman, A. and Barooah, P. (2018). Simultaneous identification of dynamic model and occupant-induced disturbance for commercial buildings. *Building and Environment*, 128(153-160). doi:https://doi.org/10.1016/j.buildenv.2017. 10.020.

Diestel, R. (2005). *Graph Theory*, volume 173 of *Graduate Texts in Mathematics*. Springer-Verlag, Heidelberg, 3 edition.

Doddi, H., Talukdar, S., Deka, D., and Salapaka, M. (2018). Data-driven identification of thermal network of multi-zone building. In *Decision and Control (CDC)*, 2018 IEEE 57th Annual Conference on. IEEE. Under review.

Duan, J., Soussen, C., Brie, D., Idier, J., Wan, M., and Wang, Y.P. (2016). Generalized lasso with under-determined regularization matrices. *Signal processing*, 127, 239–246.

Energy Information Administration (2012). 2012 commercial buildings energy consumption survey: Energy usage summary. URL https://www.eia.gov/consumption/commercial/reports/2012/energyusage/. Last accessed: April 20, 2018.

Fisk, W.J. (2000). Health and productivity gains from better indoor environments and their relationship with building

- energy efficiency. Annual Review of Energy and the Environment, 25(1), 537–566.
- Goyal, S., Liao, C., and Barooah, P. (2011). Identification of multi-zone building thermal interaction model from data. In *Decision and Control and European Control Conference* (CDC-ECC), 2011 50th IEEE Conference on, 181–186. IEEE.
- Grant, M. and Boyd, S. (2011). CVX: Matlab software for disciplined convex programming, version 1.21. http://cvxr.com/cvx.
- Hansen, P.C. (1992). Analysis of discrete ill-posed problems by means of the 1-curve. *SIAM review*, 34(4), 561–580.
- Hayden, D., Chang, Y.H., Goncalves, J., and Tomlin, C.J. (2016). Sparse network identifiability via compressed sensing. *Automatica*, 68, 9 17.
- James, G., Witten, D., Hastie, T., and Tibshirani, R. (2014). An Introduction to Statistical Learning: With Applications in R. Springer Publishing Company.
- Kim, D., Cai, J., Ariyur, K.B., and Braun, J.E. (2016). System identification for building thermal systems under the presence of unmeasured disturbances in closed loop operation: Lumped disturbance modeling approach. *Building and Environment*, 107, 169 180. doi:http://dx.doi.org/10.1016/j. buildenv.2016.07.007.
- Kim, D., Cai, J., and Braun, J.E. (2017). Identification approach to alleviate effects of unmeasured heat gains for MIMO building thermal systems. In *American Control Conference (ACC)*, 2017, 50–55.
- Madsen, H. and Hoist, J. (1995). Estimation of continuoustime models for the heat dynamics of a buildings. *Energy* and *Buildings*, 22, 67–79.
- Materassi, D., Innocenti, G., Giarr, L., and Salapaka, M. (2013). Model identification of a network as compressing sensing. *Systems & Control Letters*, 62(8), 664 672. doi: https://doi.org/10.1016/j.sysconle.2013.04.004.
- Oppenheim, A.V., Willsky, A., and Nawab, S. (1997). Signals and systems 2nd ed. *New Jersey: Prentice Hall*.
- Pendse, G.V. (2011). A tutorial on the lasso and the shooting algorithm. *Technical report, PAIN Group, Imaging and Analysis Group-McLean Hospital, Harvard Medical School*, 8.
- Penman, J.M. (1990). Second order system identification in the thermal response of a working school. *Building and Environment*, 25(2), 105–110.
- Schellen, L., Loomans, M., de Wit, M.d., Olesen, B., and van Marken Lichtenbelt, W. (2012). The influence of local effects on thermal sensation under non-uniform environmental conditionsgender differences in thermophysiology, thermal comfort and productivity during convective and radiant cooling. *Physiology & behavior*, 107(2), 252–261.
- Sensharma, N.P., Woods, J.E., and Goodwin, A.K. (1998). Relationships between the indoor environment and productivity: a literature review. *Ashrae Transactions*, 104, 686–700.
- Seppänen, O., Fisk, W.J., and Faulkner, D. (2005). Control of temperature for health and productivity in offices. *ASHRAE transactions*, 111, 680–686.
- Tom, S. (2008). Managing Energy and Comfort: Don't sacrifice comfort when managing energy. ASHRAE journal, 50(6), 18–26.
- United States Energy Information Administration (2018). Annual energy outlook. URL https://www.eia.gov/outlooks/aeo.

- Wang, S. and Xu, X. (2006). Parameter estimation of internal thermal mass of building dynamic models using genetic algorithm. *Energy conversion and management*, 47(13), 1927–1941.
- Yue, Z., Thunberg, J., Pan, W., Ljung, L., and Gonalves, J. (2017). Linear dynamic network reconstruction from heterogeneous datasets. *IFAC-PapersOnLine*, 50(1), 10586 – 10591.
- Zeng, T., Brooks, J., and Barooah, P. (2017). Simultaneous identification of linear building dynamic model and disturbance using sparsity-promoting optimization. *arXiv* preprint *arXiv*:1711.06386.